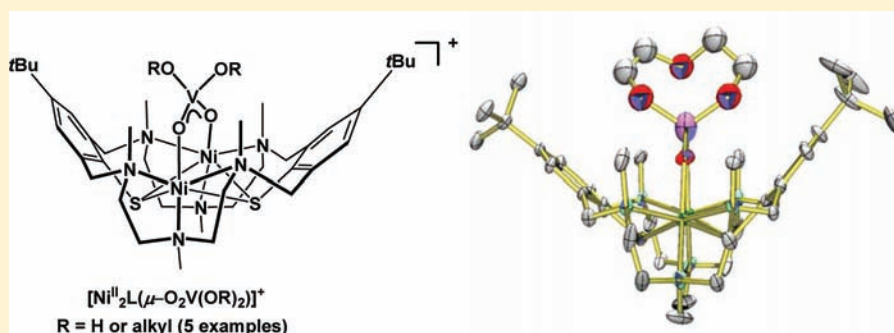


Synthesis, Structure, and Reactivity of Dinuclear Nickel Amino-Thiophenolate Complexes Bearing Bridging $\text{VO}_2(\text{OH})_2^-$ and $\text{VO}_2(\text{OR})_2^-$ Coligands

Vasile Lozan,[†] Jochen Lach, and Berthold Kersting*

Institut für Anorganische Chemie, Universität Leipzig, Johannisallee 29, D-04103 Leipzig, Germany

S Supporting Information



ABSTRACT: A series of novel mixed ligand dinickel complexes of the type $[\text{Ni}_2\text{L}(\mu\text{-L}')]^+$, where L' is a tetrahedral oxo-alkoxo vanadate ($\text{L}' = [\text{O}_2\text{V}^{\text{V}}(\text{OR})_2]^-$, R = H or alkyl) and L a macrocyclic N_6S_2 supporting ligand, have been prepared, and their esterification reactivity has been studied. The orthovanadate complex $[\text{Ni}_2\text{L}(\mu\text{-O}_2\text{V}(\text{OH})_2)]^+$ (**2**), prepared by reaction between $[\text{Ni}_2\text{L}(\mu\text{-Cl})]\text{ClO}_4$ with Na_3VO_4 and a phase transfer reagent in CH_3CN , reacts smoothly with MeOH and EtOH forming the vanadate diesters $[\text{Ni}_2\text{L}(\mu\text{-O}_2\text{V}(\text{OMe})_2)]^+$ (**3**) and $[\text{Ni}_2\text{L}(\mu\text{-O}_2\text{V}(\text{OEt})_2)]^+$ (**4**). The dialkyl orthovanadate esters in **3** and **4** are readily transesterified with mono- and difunctional alcohols. Complex **3** can also be generated from **4** by transesterification with MeOH. Complexes **3** and **4** react with diols (ethylene glycol, propylene glycol and diethylene glycol) as well to afford the complexes $[\text{Ni}_2\text{L}(\mu\text{-O}_2\text{V}(\text{OH})(\text{OCH}_2\text{CH}_2\text{OH}))]^+$ (**5**), $[\text{Ni}_2\text{L}(\mu\text{-O}_2\text{V}(\text{OCH}_2\text{CH}_2)_2)]^+$ (**6**), and $[\text{Ni}_2\text{L}(\mu\text{-O}_2\text{V}(\text{OCH}_2\text{CH}_2)_2\text{O})]$ (**7**). The crystal structures of the tetraphenylborate salts of complexes **3**–**7** reveal in each case four-coordinate $\text{O}_2\text{V}^{\text{V}}(\text{OR})_2^-$ groups bonded in a $\mu_{1,3}$ -bridging mode to generate trinuclear complexes with a central $\text{N}_3\text{Ni}(\mu\text{-S})_2(\mu_{1,3}\text{-O}_2\text{V}(\text{OR})_2)\text{NiN}_3$ core. The stabilization of the four-coordinate $\text{V}^{\text{V}}\text{O}_2(\text{OR})_2^-$ moieties is a consequence of both the two-point coordinative fixation to and the steric protection of the bowl-shape binding pocket of the $[\text{Ni}_2\text{L}]^{2+}$ fragment. Cyclic voltammetry experiments reveal that the encapsulated vanadate esters are not reduced in a potential window of -2.0 to $+2.5$ V vs SCE. The spins of the nickel(II) ($S_i = 1$ ions) in **3** are weakly ferromagnetically coupled ($J = +23$ cm^{-1} , ($\text{H} = -2J\text{S}_1\text{S}_2$)) to produce an $S = 2$ ground state.

INTRODUCTION

We and others are interested in the coordination chemistry of metal complexes with deep binding pockets, one reason being the unusual reactivities associated with confinement effects exerted by the binding cavity.^{1–13} The Robson type^{14–17} hexaaza-dithiophenolate ligand H_2L supports dinuclear transition metal complexes with a biotetrahedral $\text{N}_3\text{M}(\mu\text{-S}_2)_2(\text{L}')\text{MN}_3$ core embedded in a bowl-shaped “calixarene-like” binding pocket.^{18–20} Several unusual transformations within the pocket of the $[\text{M}_2\text{L}(\mu\text{-L}')]^+$ complexes have been reported.^{1,2} These include fixation of carbon dioxide,²¹ *cis*-bromination of α,β -unsaturated carboxylate ligands,²² highly diastereoselective Diels–Alder reactions,²³ and reduction of S_8 to S_6^{2-} by encapsulated BH_4^- .^{24,25}

Recently, we have been exploring the chemistry of first-row $[\text{M}_2\text{L}(\text{L}')^{n+}]$ complexes bearing tetrahedral main group and transition metal oxoanions as coligands L' (Figure 1). The X-ray crystal structures of the following complexes have

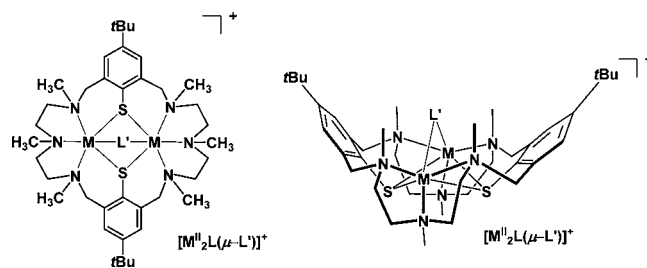


Figure 1. Lewis formula and perspective view of the structure of the $[\text{M}_2\text{L}(\mu\text{-L}')]^+$ cations.

been reported: $[\text{Ni}_2\text{L}(\mu\text{-O}_2\text{P}(\text{OH})_2)]\text{BPh}_4$,²¹ $[\text{Ni}_2\text{L}(\mu\text{-SO}_4)]$,²⁶ $[\text{Ni}_2\text{L}(\mu\text{-ClO}_4)]\text{BPh}_4$,²⁶ $[\text{Co}_2\text{L}(\mu\text{-MoO}_4)]$,²⁷ $[\text{Ni}_2\text{L}(\mu\text{-CrO}_4)]$,²⁶

Received: January 13, 2012

Published: April 24, 2012

$[\text{Ni}_2\text{L}(\mu\text{-MoO}_4)]$,²⁶ $[\text{Ni}_2\text{L}(\mu\text{-WO}_4)]$,²⁶ and $[\text{Ni}_2\text{L}(\mu\text{-ReO}_4)]\text{-}[\text{ReO}_4]$.²⁶ We have also described the synthesis and X-ray structures of two complexes with mixed oxo-alkoxo donor ligands, namely, $[\text{Co}_2\text{L}(\mu\text{-O}_2\text{Mo}(\text{OH})(\text{OMe}))]^{+27}$ and $[\text{Ni}_2\text{L}(\mu\text{-O}_2\text{P}(\text{OC}_6\text{H}_4\text{-}i\text{PrNO}_2)_2)]^{+28}$. The oxo- and oxo-alkoxo anions are all coordinated in a $\mu_{1,3}$ -bridging mode thereby generating $\text{M}_2(\mu\text{-O}_2\text{E}(\text{O})_2)$, $\text{M}_2(\mu\text{-O}_2\text{E}(\text{OR})_2)$, or $\text{M}_2(\mu\text{-O}_2\text{E}(\text{O})(\text{OR}))$ structures with two oxo, hydroxido, or alkoxo groups terminating in a hydrophobic pocket.

To further develop the coordination chemistry of these complexes, we decided to prepare and characterize $[\text{M}_2\text{L}(\mu\text{-L})]^+$ complexes bearing oxo-alkoxo vanadate ions as coligands. A literature survey reveals that relatively little is known about discrete, monomeric, four-coordinate vanadate esters.^{29,30} The vast majority of vanadate esters possess square-pyramidal or octahedral geometries at vanadium.³¹ Neutral $\text{VO}(\text{OR})_3$ alkyl esters are quite Lewis-acidic and tend to oligomerize in the solution as well as in the solid state forming five- or hexa-coordinate V^{V} compounds.^{32–34} Monomeric, four-coordinate species such as $\text{VO}(\text{O}-t\text{-Bu})_3$ appear accessible only with bulky alkoxides.^{35,36} The same is true for the anionic $\text{VO}_2(\text{OR})_2^-$ compounds. Stable species such as $[\text{VO}_2(\text{OEt})_2]^-$ do exist,^{37,38} but are difficult to isolate in their free form. It should be noted that tetrahedral oxo-alkoxo-vanadates are of biological relevance^{39–42} and industrial importance.⁴³ For example, they can act as competitive substrates to phosphodiesterases inhibiting the native enzymes.^{44,45} Oxo derivatives of vanadium play important roles in oxidative transformations of organic compounds.⁴⁶

We report here the preparation and characterization of a dinuclear nickel complex bearing the parent orthovanadate ion in its bowl-shaped binding pocket and on its selective esterification reactions to produce $[\text{Ni}_2\text{L}(\mu\text{-O}_2\text{V}(\text{OR})_2)]^+$ complexes carrying four-coordinate vanadate diesters as coligands. The spectroscopic properties, magnetic properties, results of cyclic voltammetry experiments, and the crystal structures of the complexes are also described.

EXPERIMENTAL SECTION

General Procedures. Unless otherwise noted the preparations of the metal complexes were carried out under an argon atmosphere by using standard Schlenk techniques. The compound $[\text{Ni}_2\text{L}(\mu\text{-Cl})]\text{ClO}_4$ (1ClO_4) was prepared as described in the literature.¹⁸ $\text{VO}(\text{OMe})_3$ was purchased from Aldrich. All other reagents were obtained from standard commercial sources and used without further purification.

Caution! Perchlorate salts of transition metal complexes are hazardous and may explode. Only small quantities should be prepared and great care taken.

$[\text{Ni}_2\text{L}(\mu\text{-O}_2\text{V}(\text{OH})_2)]\text{ClO}_4$ (2ClO_4) and $[\text{Ni}_2\text{L}(\mu\text{-O}_2\text{V}(\text{OH})_2)]\text{BPh}_4$ (2BPh_4). To an argon-purged solution of 1ClO_4 (92 mg, 0.10 mmol) in acetonitrile (30 mL) was added solid Na_3VO_4 (22 mg, 1.20 mmol) followed by $[\text{nBu}_4\text{N}]\text{Br}$ (38 mg, 1.20 mmol). After stirring for 2 d at room temperature, the mixture was filtered, and a solution of $\text{LiClO}_4 \cdot 3\text{H}_2\text{O}$ (32 mg, 0.20 mmol) in acetonitrile (5 mL) was added. The solution was concentrated (rotary evaporator) to about 2 mL to give a yellowish green solid, which was filtered, washed with a little cold ethanol, and dried in vacuum. Yield: 44 mg (43%). Mp 338–340 °C (decomposes without melting). IR (KBr pellet): 930 m, 925 m $\nu_3[\text{O}_2\text{V}(\text{OH})_2^-]$, 639 m $\nu_4[\text{O}_2\text{V}(\text{OH})_2^-]$; UV/vis (CH_2Cl_2 , 1.8×10^{-3} M): λ_{max} (ϵ) = 1092 (94), 920(sh, 34), 666 nm ($54 \text{ M}^{-1} \text{ cm}^{-1}$); Elemental analysis calcd (%) for $\text{C}_{38}\text{H}_{66}\text{ClN}_6\text{Ni}_2\text{O}_8\text{S}_2\text{V}$ (1002.88): C 45.51, H 6.63, N 8.38, S 6.39; found C 45.54, H 6.83, N 8.06, S 6.00. The tetraphenylborate salt 2BPh_4 was obtained by adding a solution of NaBPh_4 (342 mg, 1.00 mmol) in acetonitrile (5 mL) to a solution of 2ClO_4 (100 mg, 0.100 mmol) in acetonitrile (40 mL). The mixture

was concentrated (rotary evaporator) to about 5 mL. Upon standing for several days, a green, microcrystalline product formed. This material was filtered, washed with cold ethanol, and dried in vacuum. Yield 85 mg (70%). Mp 228–230 °C (decomposes without melting). IR (KBr pellet): 932 m, 927 m $\nu_3[\text{O}_2\text{V}(\text{OH})_2^-]$, 734s, 705s $[\text{BPh}_4^-]$, 627 m, 612 m $\nu_4[\text{O}_2\text{V}(\text{OH})_2^-]$; UV/vis (CH_2Cl_2 , 1.4×10^{-3} M): λ_{max} (ϵ) = 1092 (98), 923(sh,41), 668 nm ($54 \text{ M}^{-1} \text{ cm}^{-1}$); Elemental analysis calcd (%) for $\text{C}_{62}\text{H}_{86}\text{BN}_6\text{Ni}_2\text{O}_4\text{S}_2\text{V}$ (1222.65): C, 60.91; H, 7.09; N, 6.87; S, 5.25; found C 60.76; H 7.29; N 6.70; S 5.50.

$[\text{Ni}_2\text{L}(\mu\text{-O}_2\text{V}(\text{OCH}_3)_2)]\text{ClO}_4$ (3ClO_4) and $[\text{Ni}_2\text{L}(\mu\text{-O}_2\text{V}(\text{OCH}_3)_2)]\text{-BPh}_4$ (3BPh_4), Method A (Methanolysis of $[\text{Ni}_2\text{L}(\mu\text{-O}_2\text{V}(\text{OH})_2)]\text{-BPh}_4$ (2BPh_4)). A solution of 2BPh_4 (122 mg, 0.100 mmol) in methanol (50 mL) was stirred for 24 h at room temperature. The mixture was concentrated (rotary evaporator) to about 5 mL to give a yellowish green solid, which was filtered, washed with a little cold methanol, and dried in vacuum. The crude product was purified by recrystallization from a mixed acetonitrile/methanol (1:1) solvent system. Yield: 103 mg (82%). The presence of 3BPh_4 was ascertained by the IR band at 1306 cm^{-1} for the C–O stretch of the methoxide ligand.

Method B (Substitution of Cl^- for $\text{VO}_2(\text{OMe})_2^-$ in $[\text{Ni}_2\text{L}(\mu\text{-Cl})]\text{ClO}_4$). To a solution of $\text{VO}(\text{OCH}_3)_3$ (80 mg, 0.50 mmol) in methanol (30 mL) was added solid NaOH (20 mg, 0.50 mmol). Solid 1ClO_4 (92 mg, 0.1 mmol) was added. After stirring for 12 h at room temperature a solution of $\text{LiClO}_4 \cdot 3\text{H}_2\text{O}$ (160 mg, 1.00 mmol) in methanol (5 mL) was added. The resulting pale-green solid of 3ClO_4 was filtered, washed with cold methanol, and dried in vacuum. The crude product was purified by recrystallization from a mixed acetonitrile/methanol (1:1) solvent system. Yield: 82 mg (80%). Mp 325–326 °C (decomposes without melting). IR (KBr pellet): 1306 (O–CH₃), 1095(vs) (ClO_4^-), 940br,s $\nu_3[\text{VO}_2(\text{OMe})_2^-]$, 624 m $\nu_4[\text{ClO}_4^-]$. UV/vis (CH_2Cl_2 , 1.6×10^{-3} M): λ_{max} (ϵ) = 1092 (105), 930(sh, 25), 665 nm ($47 \text{ M}^{-1} \text{ cm}^{-1}$). Elemental analysis calcd (%) for $\text{C}_{40}\text{H}_{70}\text{ClN}_6\text{Ni}_2\text{O}_8\text{S}_2\text{V}$ (1030.93): C, 46.60; H, 6.84; N, 8.15; S, 6.22; found C 46.67; H 6.92; N 7.34; S 6.30. CV (CH_3CN , 295 K, 0.1 M $n\text{Bu}_4\text{PF}_6$, $\nu = 100 \text{ mV/s}$; $E(\text{V})$ vs SCE): $E(\text{Ni}^{\text{III}}\text{Ni}^{\text{III}}/\text{Ni}^{\text{III}}\text{Ni}^{\text{II}}) = +0.03$ ($\Delta E_p = 0.11 \text{ V}$), $E(\text{Ni}^{\text{III}}\text{Ni}^{\text{II}}/\text{Ni}^{\text{II}}\text{Ni}^{\text{II}}) = +1.54$ ($\Delta E_p = 0.117 \text{ V}$). The tetraphenylborate salt was obtained by adding a solution of NaBPh_4 (342 mg, 1.00 mmol) in methanol (10 mL) to a solution of 3ClO_4 (103 mg, 0.100 mmol) in methanol (40 mL). The green, microcrystalline product was filtered, washed with cold methanol, and dried in vacuum. Yield 115 mg (92%). Mp 228–230 °C (decomposes without melting). IR (KBr pellet): ν/cm^{-1} : 1306 (O–CH₃), 938 m, 928 m $\nu_3[\text{VO}_2(\text{OMe})_2^-]$, 734s, 705s $[\text{BPh}_4^-]$; UV/vis (CH_2Cl_2 , 1.4×10^{-3} M): λ_{max} (ϵ) = 1099 (109), 925(sh, 29), 673 (43), 311 nm ($16200 \text{ M}^{-1} \text{ cm}^{-1}$); Elemental analysis calcd (%) for $\text{C}_{64}\text{H}_{90}\text{BN}_6\text{Ni}_2\text{O}_4\text{S}_2\text{V}$ (1250.71): C, 61.46; H, 7.25; N, 6.72; S, 5.13; found C 60.96; H 7.59; N 6.63; S 4.85.

Method C (Substitution of Cl^- for H_2VO_4^- in $[\text{Ni}_2\text{L}(\mu\text{-Cl})]\text{ClO}_4$ (1ClO_4) by $\text{Na}_3\text{VO}_4/n\text{Bu}_4\text{NBr}$ Followed by Methanolysis of the Resulting $[\text{Ni}_2\text{L}(\mu\text{-O}_2\text{V}(\text{OH})_2)]\text{ClO}_4$ (2ClO_4)). To an argon-purged solution of 1ClO_4 (92 mg, 0.10 mmol) in methanol (30 mL) was added solid Na_3VO_4 (22 mg, 1.20 mmol) followed by $n\text{Bu}_4\text{NBr}$ (38 mg, 1.20 mmol). After stirring for 2 d at room temperature, the mixture was filtered, and a solution of NaBPh_4 (342 mg, 1.00 mmol) in methanol was added. The resulting green microcrystalline solid was filtered and dried in vacuum. Yield 85 mg (68%). The presence of 3BPh_4 is ascertained by the IR band at 1306 cm^{-1} for the C–O stretch of the methoxide ligand, and additionally by an X-ray crystal structure determination.

Method D (Methanolysis of $[\text{Ni}_2\text{L}(\mu\text{-O}_2\text{V}(\text{OEt})_2)]\text{BPh}_4$ (4BPh_4)). A solution of 4BPh_4 (125 mg, 0.100 mmol) in methanol (50 mL) was stirred for 24 h at room temperature. The mixture was concentrated (rotary evaporator) to about 5 mL to give a yellowish green solid, which was filtered, washed with a little cold methanol, and dried in vacuum. The crude product was purified by recrystallization from a mixed acetonitrile/methanol (1:1) solvent system. Yield: 103 mg (82%). The presence of 3BPh_4 was ascertained by the IR band at 1306 cm^{-1} for the C–O stretch of the methoxide ligand.

$[\text{Ni}_2\text{L}(\mu\text{-O}_2\text{V}(\text{OC}_2\text{H}_5)_2)]\text{BPh}_4$ (4BPh_4), Method A (Ethanolsynthesis of $[\text{Ni}_2\text{L}(\mu\text{-O}_2\text{V}(\text{OH})_2)]\text{BPh}_4$ (2BPh_4)). Compound 2BPh_4 (125 mg,

0.100 mmol) was dissolved in CH₃CN (30 mL). Ethanol (20 mL) was added. After stirring for 12 h, the mixture was concentrated (rotary evaporator) to about 5 mL to give a yellowish green solid, which was filtered, washed with a little cold ethanol, and dried in vacuum. Yield: 104 mg (81%). Mp 240–242 °C (decomposes without melting). IR (KBr pellet): ν/cm^{-1} : 1314 (O–CH₂CH₃), 936 m, 927 m $\nu_3[\text{VO}_2(\text{OEt})_2^-]$, 734s, 705s [BPh₄⁻]; UV/vis (CH₂Cl₂, 1.5 × 10⁻³ M): $\lambda_{\text{max}}(\epsilon) = 1086$ (101), 926sh (31), 668 (44), 310 nm (16400 M⁻¹ cm⁻¹); Elemental analysis calcd (%) for C₆₆H₉₄BN₆Ni₂O₄S₂V (1278.76): C 61.99, H 7.41, N 6.57, S 5.02; found C 61.46, H 7.31, N 6.49, S 4.83. Crystals of [Ni₂L(μ-O₂V(OC₂H₅)₂)]BPh₄·xMeCN (4BPh₄·xMeCN) suitable for X-ray crystallography were picked from the mother liquor.

Method B (Ethanolysis of [Ni₂L(μ-O₂V(OMe)₂)]BPh₄ (3BPh₄)). A solution of 3BPh₄ (125 mg, 0.100 mmol) in ethanol (50 mL) was stirred for 24 h at room temperature. The mixture was concentrated (rotary evaporator) to about 10 mL to give a yellowish green solid, which was filtered, washed with a little cold ethanol, and dried in vacuum. The crude product was purified by recrystallization from a mixed acetonitrile/ethanol (1:1) solvent system. Yield: 103 mg (82%). The presence of 4BPh₄ can be readily ascertained by the new IR band at 1314 cm⁻¹ for the C–O stretch of the ethoxide ligand.

Method C (Substitution of Cl⁻ for H₂VO₄⁻ in [Ni₂L(μ-Cl)]ClO₄ (1ClO₄) Followed by Ethanolysis of the Resulting [Ni₂L(μ-O₂V(OH)₂)]ClO₄ (2ClO₄)). To an argon-purged solution of [Ni₂L(μ-Cl)]ClO₄ (92 mg, 0.10 mmol) in ethanol (30 mL) was added solid Na₃VO₄ (22 mg, 1.20 mmol) followed by [*n*Bu₄N]Br (38 mg, 1.20 mmol). After stirring for 2 d at room temperature, the mixture was filtered, and a solution of NaBPh₄ (342 mg, 1.00 mmol) in ethanol was added. The resulting green microcrystalline solid was filtered and dried in vacuum. Yield 92 mg (72%). The identity of 4BPh₄ prepared by method C was ascertained by the presence of the IR band at 1314 cm⁻¹ for the C–O stretch of the ethoxide ligand and the absence of the 1306 cm⁻¹ band for the methoxide ligand. The identity of this material was also ascertained by an X-ray crystal structure determination.

[Ni₂L(μ-O₂V(OH)(OCH₂CH₂OH))]BPh₄ (5BPh₄). This compound was prepared by method B as described for 3BPh₄. Compound 2BPh₄ (125 mg, 0.100 mmol) was dissolved in CH₃CN (30 mL). Ethylene glycol (20 mL) was added. After stirring for 12 h, the mixture was concentrated (rotary evaporator) to about 5 mL to give a yellowish green solid, which was filtered, washed with a little cold ethanol, and dried in vacuum. Yield: 78 mg (62%). Mp 236–238 °C (decomposes without melting). IR (KBr pellet): 936 m, 913 m $\nu_3[\text{O}_2\text{V}(\text{OH})(\text{OCH}_2\text{CH}_2\text{OH})^-]$, 735s, 704s [BPh₄⁻]; UV/vis (CH₂Cl₂, 1.5 × 10⁻³ M): $\lambda_{\text{max}}(\epsilon) = 1088$ (111), 918sh (28), 667 (57), 315 nm (15870 M⁻¹ cm⁻¹); Elemental analysis calcd (%) for C₆₄H₉₀BN₆Ni₂O₅S₂V (1266.71): C 60.68, H 7.16, N 6.63, S 5.06; found C 60.79, H 7.44, N 6.81, S 4.78.

[Ni₂L(μ-O₂V(OCH₂)₂CH₂)]BPh₄ (6BPh₄). This compound was prepared by method B as detailed above for 3BPh₄. Compound 2BPh₄ (125 mg, 0.100 mmol) was dissolved in CH₃CN (30 mL). 1,3-Propanediol (20 mL) was added. After stirring for 12 h, the mixture was concentrated (rotary evaporator) to ~5 mL to give a yellowish green solid, which was filtered, washed with a little cold ethanol, and dried in vacuum. Yield: 86 mg (68%). Mp 235–237 °C (decomposes without melting). IR (KBr pellet): 945 m, 927 m $\nu_3[\text{O}_2\text{V}(\text{OCH}_2)_2\text{CH}_2^-]$, 734s, 705s [BPh₄⁻]; UV/vis (CH₂Cl₂, 1.5 × 10⁻³ M): $\lambda_{\text{max}}(\epsilon) = 1084$ (96), 932sh (25), 667 (48), 312 nm (15900 M⁻¹ cm⁻¹); Elemental analysis calcd (%) for C₆₅H₉₀BN₆Ni₂O₄S₂V (1262.72): C 61.83, H 7.18, N 6.66, S 5.08; found C 62.02, H 7.23, N 6.78, S 5.08.

[Ni₂L(μ-O₂V(OCH₂CH₂)₂O)]BPh₄ (7BPh₄). This compound was prepared by method B detailed above for 3BPh₄. Compound 2BPh₄ (125 mg, 0.100 mmol) was dissolved in CH₃CN (30 mL). Diethylene glycol (20 mL) was added. After stirring for 12 h, the mixture was concentrated (rotary evaporator) to about 5 mL to give a yellowish green solid, which was filtered, washed with a little cold ethanol, and dried in vacuum. Yield: 95 mg (73%). Mp 241–243 °C (decomposes without melting). IR (KBr pellet): 933 m, 910 m

$\nu_3[\text{O}_2\text{V}(\text{OCH}_2\text{CH}_2)_2\text{O}^-]$, 732s, 705s [BPh₄⁻]; UV/vis (CH₂Cl₂, 1.5 × 10⁻³ M): $\lambda_{\text{max}}(\epsilon) = 1089$ (113), 925sh (22), 669 (53), 312 nm (15900 M⁻¹ cm⁻¹); Elemental analysis calcd (%) for C₆₆H₉₂BN₆Ni₂O₅S₂V (1292.74): C 61.32, H 7.17, N 6.50, S 4.96; found C 61.22, H 7.11, N 6.86, S 5.18.

CRYSTAL STRUCTURE DETERMINATIONS

Single crystals of 3BPh₄·xMeCN–7BPh₄·xMeCN suitable for X-ray structure analysis were grown by recrystallization from acetonitrile. The crystals were mounted on glass fibers using perfluoropolyether oil. Intensity data were collected at 210(2) K, using a Bruker SMART CCD diffractometer. Graphite monochromated Mo-K_α radiation ($\lambda = 0.71073 \text{ \AA}$) was used throughout. The data were processed with SAINT and corrected for absorption using SADABS.⁴⁷ The structures were solved by direct methods using the program SHELXS-86⁴⁸ and refined by full-matrix least-squares techniques against *F*² using SHELXL-97.⁴⁹ The ShelXTL version 5.10 program package was used for the structure solutions and refinements.⁵⁰ PLATON was used to search for higher symmetry.⁵¹ Ortep3 was used for the artwork of the structures.⁵² Hydrogen atoms were included in calculated positions with their bonding distances and thermal parameters 1.2 times (1.5 times for CH₃ groups) the thermal parameter of the atoms to which they were attached. Selected details of the data collection and refinement are given in Tables 2 and 3.

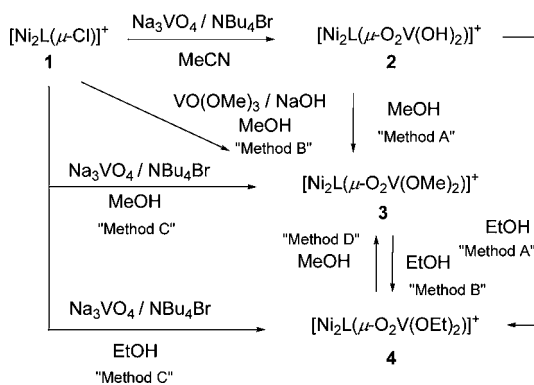
The exact number of the acetonitrile molecules, which are heavily disordered in all structures, could not be determined. Electron density attributed to heavily disordered acetonitrile molecules was removed from the structure (and the corresponding *F*_o) with the Squeeze procedure implemented in the Platon program suite.⁵³

In the crystal structure of [Ni₂L(μ-O₂V(OCH₂)₂CH₂)]·BPh₄·xCH₃CN (6BPh₄·xCH₃CN), one *tert*-butyl group was found to be disordered over two positions. A split atom model was applied to account for this disorder. The site occupancies of the two orientations were refined as 0.71(2) (for C36a–C38a) and 0.29(2) (for C36b–C38b).

Physical Measurements. Melting points were determined in open glass capillaries and are uncorrected. Elemental analysis were performed on a Vario EL analyzer (Elementaranalysensysteme GmbH). IR spectra were taken on a Bruker Tensor 27 FT-IR-spectrophotometer as KBr pellets. The electronic absorption spectra were measured on a Jasco V-570 UV/vis/NIR spectrometer. Cyclic voltammetry measurements were carried out at 25 °C with an EG&G Princeton Applied Research potentiostat/galvanostat model 263 A. The cell contained a Pt working electrode, a Pt wire auxiliary electrode, and a Ag wire as reference electrode. Concentrations of solutions were 0.10 M in supporting electrolyte [(*n*-Bu)₄N]PF₆ and about 1.0 × 10⁻³ M in sample. Cobaltocenium hexafluorophosphate (Cp₂CoPF₆) was used as internal standard. All potentials were converted to the SCE reference using tabulated values.⁵⁴ The temperature-dependent magnetic susceptibility measurement was carried out using a MPMS 7XL SQUID magnetometer (Quantum Design) over the temperature range from 2–330 K at an applied magnetic field of 0.5 T. The observed susceptibility data were corrected for underlying diamagnetism.

RESULTS AND DISCUSSION

Syntheses and Reactions of the Complexes. The synthesized compounds and procedures are shown in Scheme 1.

Scheme 1. Synthesis of Complexes 2–4^a

^aThe cations were isolated as ClO_4^- and/or BPh_4^- salts.

Initial attempts targeted the synthesis of the orthovanadate complex $[\text{Ni}_2\text{L}(\mu\text{-O}_2\text{V}(\text{OH})_2)]^+$ (2) applying a method used for the dihydrogen phosphate complex $[\text{Ni}_2\text{L}(\mu\text{-O}_2\text{P}(\text{OH})_2)]^+$.²¹ Thus, $[\text{Ni}_2\text{L}(\mu\text{-Cl})]^+$ (1) was treated in MeOH with solid Na_3VO_4 and $n\text{Bu}_4\text{NBr}$ acting as a phase transfer agent to solubilize the vanadate ion, but this resulted in the formation of the dimethyl orthovanadate complex $[\text{Ni}_2\text{L}(\mu\text{-O}_2\text{V}(\text{OMe})_2)]^+$ (3), most likely via solvolysis of an intermediate dihydrogen vanadate complex $[\text{Ni}_2\text{L}(\mu\text{-O}_2\text{V}(\text{OH})_2)]^+$ (2) (Scheme 1, Method C). Esterification reactions of vanadate with alcohols are well-documented in the literature.^{55–61} We sought to trap the dihydrogen vanadate intermediate 2 by carrying out the reaction in acetonitrile. Indeed, a green solution forms indicative of a successful substitution reaction, and the desired complex 2 with an encapsulated orthovanadate moiety can be isolated as a yellowish-green ClO_4^- (or BPh_4^-) salt in good yields.

In the absence of protic reagents 2ClO_4^- or 2BPh_4^- are stable for weeks both in the solid state and in solution. This stability is quite remarkable given that vanadate readily undergoes condensation reactions forming polynuclear oxo-vanadates.^{62,63} The inhibition of condensation reactions by confinement has precedence in the literature. Fujita, for example, has reported on the stabilization of a cyclic trisilanol in the pocket of a coordination cage.⁶⁴

The successful isolation of the dihydrogen vanadate complex 2 allowed us to examine its solvolysis reaction with alcohols. Indeed, when 2BPh_4^- is dissolved in MeOH methanolysis occurs and the dimethyl vanadate complex 3 can be isolated in nearly quantitative yield as the BPh_4^- salt (Method A). We also examined the possibility of a reaction of 1 with $\text{O}_2\text{V}(\text{OMe})_2^-$ (prepared in situ from $\text{VO}(\text{OMe})_3 + \text{NaOH}$). In fact, this also provides 3 in good yield, showing that a substitution reaction of the bridging chloride in 1 with a $\text{O}_2\text{V}(\text{OMe})_2^-$ unit can take place as well (Method B). It was appropriate to investigate whether the diester 3 would undergo a transesterification reaction in ethanol. When 3BPh_4^- is stirred in EtOH ethanolysis occurs and the diethyl orthovanadate ester 4 can be obtained as a pale-green microcrystalline 4BPh_4^- salt (Method B). Complex 4BPh_4^- is also accessible from 1 or 2 by the other methods detailed above for 3BPh_4^- . Finally, 3BPh_4^- could also be regenerated from 4BPh_4^- by solvolysis with MeOH (Method D).

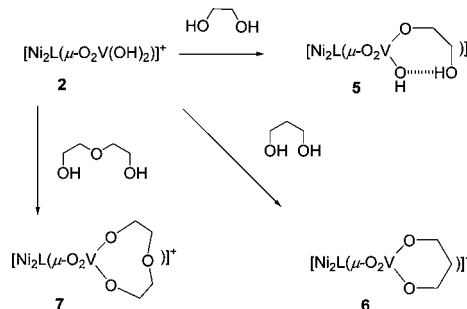
The smooth solvolysis reactions of the above vanadate esters in 2–4 contrasts the behavior of the dihydrogenphosphate in $[\text{Ni}_2\text{L}(\mu\text{-O}_2\text{P}(\text{OH})_2)]\text{BPh}_4^-$ and the bis(para-nitrophenolate)phosphate

in $[\text{Ni}_2\text{L}(\mu\text{-O}_2\text{P}(\text{OC}_6\text{H}_4\text{-}p\text{NO}_2)_2)]^+$,²⁸ which are both unreactive in solvolysis reactions. This fact is attributable to the ability of vanadium(V) to adopt higher coordination numbers than 4 thereby easing the coordination of an attacking alcohol. Attempts to monitor the reactions by NMR spectroscopy were not successful. The ^1H and ^{13}C NMR spectra are featureless, attributable to the presence of paramagnetic compounds.⁶⁵ This is supported by the magnetic properties of 3BPh_4^- (see below).

The stabilization of monomeric, four-coordinate oxovanadium alkoxides has precedence in the literature, and can be achieved with bulky alkoxides such as phenol, adamantanol, or norborneol.⁶⁶ The latter two show much slower ester hydrolysis reactions than sterically less encumbered vanadate esters, and were shown to prevent association around the small vanadium atom.

To see, whether five-coordinate vanadate esters can be accommodated in the binding pocket of the $[\text{Ni}_2\text{L}]^{2+}$ fragment, we performed transesterification reactions of 2BPh_4^- with ethylene glycol, propane-1,3-diol, and diethylene glycol. Such diols are known to form five-coordinate oxovanadium alkoxides.^{67–69} The reactions were run in the neat solvents (Scheme 2). In the case of ethylene glycol, only one OH

Scheme 2. Preparation of Complexes 5–7



group reacts, and complex 5 (isolated as BPh_4^- salt) forms as the sole product. The formation of the mono ester rather than the chelate is attributable to the constraints of the glycol unit preventing it from forming a five-membered ring with the tetrahedral V^{V} ion and vice versa. Gresser and Tracey have studied the esterification of ethylene glycol by vanadate in aqueous solution.⁷⁰ At least three species, 2-hydroxyethyl vanadate, bis(2-hydroxyethyl) vanadate, and dimeric $(\text{CH}_2\text{O})_2(\text{O})(\text{OH})\text{V}-\text{O}-\text{V}(\text{O})(\text{OH})(\text{OCH}_2)_2$, have been identified by vanadium-51 NMR spectroscopy. The selective formation of 5 is attributable to trapping of the 2-hydroxyethyl vanadate species from solution.

The other two diols with longer alkyl chains produce the cyclic esters $[\text{Ni}_2\text{L}(\mu\text{-O}_2\text{V}(\text{OCH}_2)_2\text{CH}_2)]^+$ (6) and $[\text{Ni}_2\text{L}(\mu\text{-O}_2\text{V}(\text{OCH}_2\text{CH}_2)_2\text{O})]^+$ (7). Unconstrained reactions between vanadate precursors and diols produce are less selective. VOCl_3 , for example, reacts with propane-1,3-diol to produce tetrameric vanadium(V) clusters.⁷¹ The present examples are obviously less complex than unconstrained esterifications of alcohols by vanadate. The results imply that the binding pocket of the $[\text{Ni}_2\text{L}]^{2+}$ fragment is too small to accommodate a five-coordinated oxovanadate ester.

Spectroscopic Characterization of the Complexes. The synthesized compounds gave satisfactory elemental analyses and were further characterized by IR and UV/vis-spectroscopy,

cyclic voltammetry (in the case of 3ClO_4), temperature dependent magnetic susceptibility measurements (for 3BPh_4), and X-ray structure analysis.

The IR spectra of complexes **2–7** are very similar. The most prominent features are the two bands in the $970\text{--}950\text{ cm}^{-1}$ region (see Table 1), which are tentatively assigned to the

Table 1. Selected Spectroscopic Data for **2–7**

| compd. | coligand | IR, ν / (cm^{-1}) ^a | UV/vis, λ /nm ($\epsilon/\text{M}^{-1}\text{ cm}^{-1}$) ^{b,c} |
|-------------------------|---|--|---|
| | | $\nu_3[\text{VO}_4]$ | ν_2, ν_1 |
| 2 ClO_4 | $[\mu\text{-O}_2\text{V}(\text{OH})_2]^-$ | 930 m, 925 m | 666 (55), 920(sh, 34), 1092(94) |
| 2 BPh_4 | $[\mu\text{-O}_2\text{V}(\text{OH})_2]^-$ | 932 m, 927 m | 668 (54), 923(sh, 41), 1092 (98) |
| 3 ClO_4 | $[\mu\text{-O}_2\text{V}(\text{OMe})_2]^-$ | 940 br,s | 665 (47), 930(sh, 25), 1092 (105) |
| 3 BPh_4 | $[\mu\text{-O}_2\text{V}(\text{OMe})_2]^-$ | 938 m, 928 m | 673(43), 925(sh, 29), 1099(109) |
| 4 BPh_4 | $[\mu\text{-O}_2\text{V}(\text{OEt})_2]^-$ | 936 m, 927 m | 668 (44), 926(sh, 31), 1086 (101) |
| 5 BPh_4 | $[\mu\text{-O}_2\text{V}(\text{OH})(\text{O}(\text{CH}_2)_2\text{OH})]^-$ | 936 m, 913 m | 667 (57), 918(sh, 28), 1088 (111) |
| 6 BPh_4 | $[\mu\text{-O}_2\text{V}(\text{OCH}_2)_2\text{CH}_2]^-$ | 945 m, 927 m | 667(48), 932(sh, 25), 1084(96) |
| 7 BPh_4 | $[\mu\text{-O}_2\text{V}(\text{OCH}_2\text{CH}_2)_2\text{O}]^-$ | 933 m, 910 m | 669(53), 925(sh, 22), 1089(113) |

^aAs KBr pellet. ^bSolvent: CH_2Cl_2 ; Concentration: $\sim 10^{-3}$ M. ^csh = shoulder.

$\nu_3(\text{VO}_4)$ stretching mode of the dialkoxy vanadates. The splitting of the ν_3 mode is attributed to the lowering of the symmetry from T_d to local C_{2v} (or lower) symmetry. For the dihydrogen vanadate complex **2** BPh_4 , a weak band at 3522 cm^{-1} is tentatively assigned to the O–H stretching vibration of the terminal hydroxide ligand.

UV/vis Spectroscopy. The UV/vis spectra of the perchlorate (or tetraphenylborate) salts of **2–7** were registered in CH_2Cl_2 solution. The intense absorptions below 500 nm can be attributed to $\pi\text{--}\pi^*$ transitions within the aromatic rings of the supporting ligands or to thiolate to nickel ($\text{RS}^- \rightarrow \text{Ni}^{\text{II}}$) charge-transfer bands, normal for $[\text{Ni}_2\text{L}(\text{L}')^+]^+$ complexes.⁷² Above 500 nm there are two well-defined bands at ~ 670 and 1090 nm attributable to the spin-allowed d-d-transitions of a six-coordinate nickel(II) ion (assigned as ${}^3\text{A}_{2g} \rightarrow {}^3\text{T}_{1g}$, ${}^3\text{A}_{2g} \rightarrow {}^3\text{T}_{2g}$ in pure octahedral symmetry). There is also a weak shoulder around 920 nm flanking the ν_1 transition. This is attributed to a spin-forbidden ${}^3\text{A}_{2g} \rightarrow {}^1\text{E}_g(\text{D})$ transition. It is indicative of the presence of a significant distortion from O_h symmetry. The ${}^3\text{A}_{1g} \rightarrow {}^3\text{T}_{1g}(\text{P})$ transition expected for Ni^{II} ($S = 1$) is obscured in each case by the strong $\text{RS}^- \rightarrow \text{Ni}^{\text{II}}$ charge transfer (CT) transitions. The ν_1 value of 1092 nm corresponds to an octahedral splitting parameter Δ_o of 9158 cm^{-1} . This is a typical value for $[\text{Ni}_2\text{L}(\mu\text{-EO}_4)]^+$ complexes bearing tetrahedral oxoanions.²⁶

Cyclic Voltammetry. Given the rich redox-chemistry of vanadium it was of interest to determine the redox properties of the $[\text{Ni}_2\text{L}(\text{O}_2\text{V}(\text{OR})_2)]^+$ complexes. Figure 2 shows the cyclic voltammogram of the dimethyl vanadate ester **3** ClO_4 in CH_3CN which is representative for all compounds.

Two waves, one at $E_{1/2}^1 = +0.03$ versus SCE with a peak-to-peak separation ΔE_p of 0.110 V and one at $E_{1/2}^2 = +1.54$ with $\Delta E_p = 0.117$ V, are observed. These oxidations are very similar to those of the carboxylato bridged $[\text{Ni}_2\text{L}(\text{O}_2\text{CMe})]^+$ complex

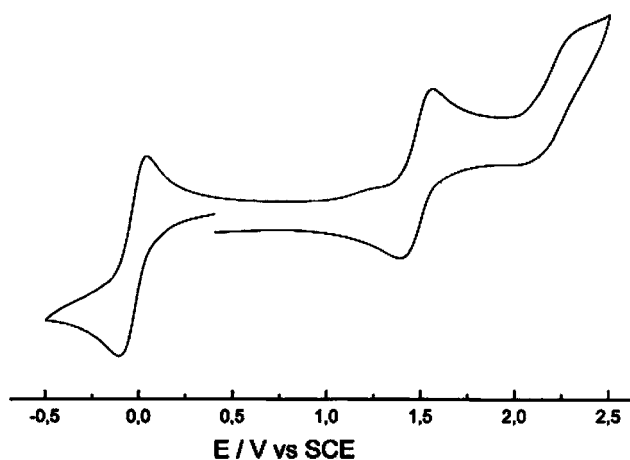
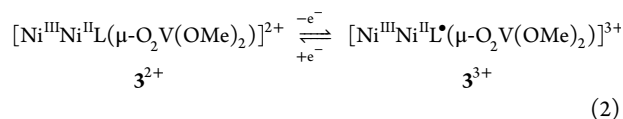
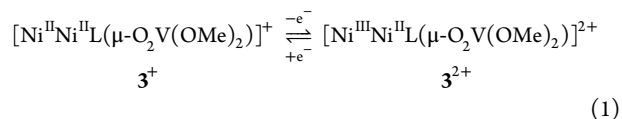


Figure 2. Cyclic voltammogram of **3** ClO_4 in CH_3CN at 298 K. Experimental conditions: 0.1 M $[\text{n-Bu}_4\text{N}][\text{PF}_6]$, about 1×10^{-3} M sample concentration, Pt disk working electrode, Ag wire reference electrode, scan rate 100 mV/s, $[\text{Co}(\text{Cp}_2)]\text{PF}_6$ internal reference.

reported earlier.⁷³ The redox waves are accordingly assigned to metal-centered and ligand-based oxidations within the $[\text{Ni}_2\text{L}]^{2+}$ unit as represented in eqs 1 and 2. In our potential window ranging from -2.0 to $+2.5$ V vs SCE, however, further redox waves are not observed. It can be said that the $\text{O}_2\text{V}(\text{OMe})_2^-$ unit is redox inactive in this potential range. The redox behavior of the present dialkyl vanadates is similar to those of four-coordinate oxovanadium alkoxides stabilized by bulky alkoxides. $\text{VO}(\text{O-1-Ad})_3$ (Ad = Adamantyl), for example, is redox inactive down to -2.3 V (in THF).⁶⁵ This would support the observed stabilization to be mainly steric in nature.



Magnetic Properties. Temperature-dependent magnetic susceptibility measurements for the compound **3** BPh_4 were carried out to study the magnetic properties of the trinuclear $\text{Ni}^{\text{II}}_2\text{V}^{\text{V}}$ complexes. The temperature-dependent susceptibility data for a powdered sample of **3** BPh_4 were measured between 2 and 330 K using a MPMS 7XL SQUID magnetometer (Quantum Design) in an applied external magnetic field of 0.5 T. Figure 3 displays the temperature dependence of the molar magnetic susceptibility (per dinuclear complex), in the form of a $\chi_M T$ versus T plot for **3** BPh_4 . The value of $\chi_M T$ increases from $2.73\text{ cm}^3\text{ K mol}^{-1}$ ($4.68\ \mu_B$) at 330 K to a maximum value of $3.56\text{ cm}^3\text{ K mol}^{-1}$ ($5.34\ \mu_B$) at 20 K, and then decreases to $2.71\text{ cm}^3\text{ K mol}^{-1}$ ($4.66\ \mu_B$) at 2 K. This behavior indicates an intramolecular ferromagnetic exchange interaction between the two Ni^{II} ions that leads to an $S = 2$ ground state of the complex. The decrease in μ_B below 20 K is presumably due to zero-field splitting of Ni^{II} and/or saturation effects.

We simulated the temperature dependence of the magnetic data of complex **3** BPh_4 by using the appropriate spin-Hamiltonian (eq 3)^{74,75} which contains a Zeeman and a zero-field splitting term by using a full-matrix diagonalization

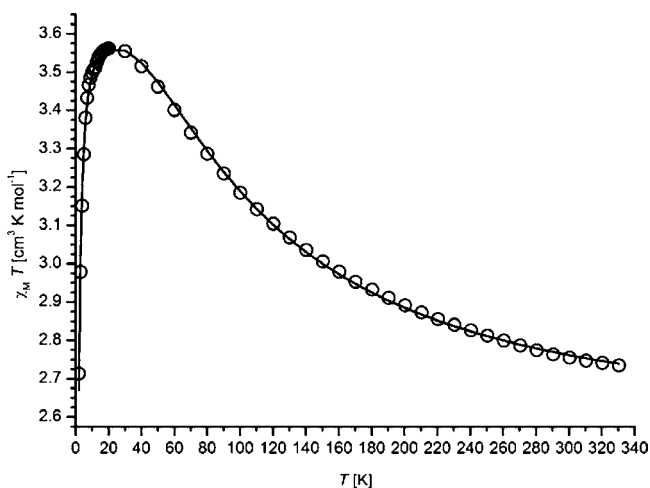


Figure 3. Temperature dependence of $\chi_M T$ for 3BPh₄ (per dinuclear complex). The full line represents the best theoretical fit to eq 3. Experimental and calculated values are provided as Supporting Information.

approach. The introduction of a D parameter is appropriate for octahedral Ni^{II}, since the noncubic components of the ligand field may act on the ³A_{2g} ground state to produce a zero-field splitting which may be of the same order of magnitude as J .^{76,77}

$$H = -2JS_1S_2 + \sum_{i=1}^2 [D_i(\hat{S}_{iz}^2 - \frac{1}{3}S_i(S_i + 1)) + g_i\mu_B B_\tau \hat{S}_{i\tau}]$$

$$(\tau = x, y, z) \quad (3)$$

By taking into account the zero-field splitting and temperature independent paramagnetism,⁷⁸ a good fit of the experimental data, shown in Figure 3 as a solid line, was possible over the full temperature range, yielding $J = +23 \text{ cm}^{-1}$,

$g = 2.19$, $TIP = 1.60 \times 10^{-4} \text{ cm}^3 \text{ mol}^{-1}$, and $|D| = 7.22 \text{ cm}^{-1}$. The latter value should be taken as indicative rather than definite, because temperature dependent magnetic susceptibility measurements are not very appropriate for the determination of D .⁷⁹ Nevertheless, J is not influenced markedly by the value of D and represents an accurate measure of the magnetic coupling in this complex. The J and g values determined for 3BPh₄ are quite similar to other bioctahedral [Ni₂L(L')]⁺ complexes coligated by $\mu_{1,3}$ -bridging oxoanions (e.g., $J = +21.7 \text{ cm}^{-1}$ for [Ni₂L(OAc)]⁺,⁸⁰ $J = +24.8 \text{ cm}^{-1}$ for [Ni^{II}₂L(O₂SO₂)]⁺.²⁶

Description of the Crystal Structures. The X-ray crystal structures of [Ni₂L(μ-O₂V(OMe)₂)]BPh₄·*x*MeCN, (3BPh₄·*x*MeCN),⁸¹ [Ni₂L(μ-O₂V(OEt)₂)]BPh₄·*x*MeCN, (4BPh₄·*x*MeCN), [Ni₂L(μ-O₂V(OH)(OCH₂CH₂OH))]BPh₄·*x*MeCN, (5BPh₄·*x*MeCN), [Ni₂L(μ-O₂V(OCH₂)₂CH₂)]BPh₄·*x*MeCN, (6BPh₄·*x*MeCN), and [Ni₂L(μ-O₂V(OCH₂CH₂)₂O)]BPh₄·*x*MeCN (7BPh₄·*x*MeCN) were determined to ascertain the composition and structures of the complexes. Experimental crystallographic data are summarized in Tables 2 and 3. Selected bond lengths and angles are given in Table 4. A common labeling scheme for the [Ni₂L(μ-O₂V(OR)₂)]⁺ complexes has been used to facilitate structural comparisons. Further data are available as Supporting Information.

[Ni₂L(μ-O₂V(OMe)₂)]BPh₄·*x*MeCN (3BPh₄·*x*MeCN) and [Ni₂L(μ-O₂V(OEt)₂)]BPh₄·*x*MeCN (4BPh₄·*x*MeCN).⁸¹ Pale green crystals of the title compounds suitable for X-ray diffraction analysis were obtained by slow evaporation from mixed acetonitrile/methanol (1:1) solutions. The structure of 3BPh₄·*x*CH₃CN is representative for the two compounds. It consists of cationic [Ni₂L(μ-O₂V(OMe)₂)]⁺ complexes, tetraphenylborate anions and CH₃CN solvate molecules.⁸¹ There are no intermolecular interactions between the components. ORTEP views of the molecular structures of the two [Ni₂L(μ-O₂V(OR)₂)]⁺ cations are shown in Figures 4 and 5.

Table 2. Selected Crystallographic Data for [Ni₂L(μ-O₂V(OMe)₂)]BPh₄·*x*MeCN (3BPh₄·*x*MeCN), [Ni₂L(μ-O₂V(OEt)₂)]BPh₄·*x*MeCN (4BPh₄·*x*MeCN), and [Ni₂L(μ-O₂V(OH)(OCH₂CH₂OH))]BPh₄·*x*MeCN (5BPh₄·*x*MeCN)^a

| | 3BPh ₄ · <i>x</i> MeCN ^a | 4BPh ₄ · <i>x</i> MeCN ^a | 5BPh ₄ · <i>x</i> MeCN ^a |
|---|---|---|---|
| formula | C ₆₄ H ₉₀ BN ₆ Ni ₂ O ₄ S ₂ V | C ₆₆ H ₉₄ BN ₆ Ni ₂ O ₄ S ₂ V | C ₆₄ H ₉₀ BN ₆ Ni ₂ O ₄ S ₂ V |
| <i>M_r</i> [g/mol] | 1250.71 | 1278.76 | 1266.71 |
| space group | <i>P</i> 2 ₁ / <i>n</i> | <i>P</i> $\bar{1}$ | <i>P</i> $\bar{1}$ |
| <i>a</i> , Å | 16.108(3) | 16.065(3) | 15.862(4) |
| <i>b</i> , Å | 28.455(6) | 16.184(3) | 16.098(4) |
| <i>c</i> , Å | 16.291(3) | 16.414(3) | 16.444(4) |
| α , deg | 90.00 | 64.20(3) | 64.320(4) |
| β , deg | 113.27(3) | 72.01(3) | 72.381(4) |
| γ , deg | 90.00 | 66.63(3) | 66.616(5) |
| <i>V</i> , Å ³ | 6860(2) | 3479(1) | 3429.7(13) |
| <i>Z</i> | 4 | 2 | 2 |
| <i>T</i> /K | 213 | 213 | 213 |
| <i>D</i> _{calcd} , g/cm ³ | 1.211 | 1.221 | 1.227 |
| μ (Mo <i>K</i> α), mm ⁻¹ | 0.784 | 0.775 | 0.786 |
| <i>R</i> 1 ^b | 0.0759 | 0.0593 | 0.0823 |
| <i>wR</i> 2 ^c | 0.1659 | 0.1714 | 0.2114 |
| max, min peaks, e/Å ³ | 0.567, -0.904 | 1.370, -1.966 | 0.646, -1.590 |

^aThe acetonitrile solvate molecules are heavily disordered and the exact number of the solvate molecules could not be determined. Electron density attributed to heavily disordered acetonitrile molecules was removed from the structures (and the corresponding F_o) with the Squeeze procedure implemented in the Platon program suite, see Experimental Section. ^b $R1 = \sum \|F_o\| - \|F_c\| / \sum \|F_o\|$. Observation criterion: $I > 2\sigma(I)$. ^c $wR2 = \{ \sum [w(F_o^2 - F_c^2)^2] / \sum [w(F_o^2)^2] \}^{1/2}$.

Table 3. Selected Crystallographic data for $[\text{Ni}_2\text{L}(\mu\text{-O}_2\text{V}(\text{OCH}_2)_2\text{CH}_2)]\text{BPh}_4 \cdot x\text{MeCN}$ (**6BPh₄·xMeCN**) and $[\text{Ni}_2\text{L}(\mu\text{-O}_2\text{V}(\text{OCH}_2\text{CH}_2)_2\text{O})]\text{BPh}_4 \cdot x\text{MeCN}$ (**7BPh₄·xMeCN**)^a

| | 6BPh ₄ ·xMeCN ^a | 7BPh ₄ ·xMeCN ^a |
|--|---|---|
| formula | C ₆₅ H ₉₀ BN ₆ Ni ₂ O ₄ S ₂ V | C ₆₆ H ₉₂ BN ₆ Ni ₂ O ₅ S ₂ V |
| M _r [g/mol] | 1262.72 | 1292.75 |
| space group | P $\bar{1}$ | P $\bar{1}$ |
| a, Å | 15.915(3) | 16.016(2) |
| b, Å | 16.087(3) | 16.114(2) |
| c, Å | 16.577(3) | 16.455(2) |
| α, deg | 64.639(3) | 64.009(3) |
| β, deg | 72.342(3) | 72.197(3) |
| γ, deg | 66.256(3) | 66.462(3) |
| V, Å ³ | 3466(1) | 3455.3(8) |
| Z | 2 | 2 |
| T/K | 213 | 213 |
| D _{calcd} , g/cm ³ | 1.210 | 1.243 |
| μ(Mo Kα), mm ⁻¹ | 0.777 | 0.782 |
| R1 ^b | 0.0551 | 0.0888 |
| wR2 ^c | 0.1216 | 0.2271 |
| max, min peaks, e/Å ³ | 0.647/−0.696 | 1.204/−1.739 |

^aThe acetonitrile solvate molecules are heavily disordered, and the exact number of the solvate molecules could not be determined. Electron density attributed to heavily disordered acetonitrile molecules was removed from the structures (and the corresponding F_o) with the Squeeze procedure implemented in the Platon program suite, see Experimental Section. ^b $R1 = \sum ||F_o| - |F_c|| / \sum |F_o|$. Observation criterion: $I > 2\sigma(I)$. ^c $wR2 = \{ \sum [w(F_o^2 - F_c^2)^2] / \sum [w(F_o^2)^2] \}^{1/2}$.

The $\text{VO}_2(\text{OMe})_2^-$ in $[\text{Ni}_2\text{L}(\mu\text{-O}_2\text{V}(\text{OMe})_2)]^+$ coordinates in a bidentate bridging mode. The supporting amino-thiophenolate ligand adopts a bowl-shaped, “calixarene-like” cone conformation, a situation typical for $[\text{Ni}^{\text{II}}_2\text{L}(\text{L}')^+]^+$ complexes coligated by $\mu_{1,3}$ -bridging oxoanions.²⁶ The coordination environment about the vanadium atom is not perfectly tetrahedral, as already inferred from IR spectroscopy. The V–O bonds vary from 1.615(5) Å to 1.825(7) Å, and the O–V–O bond angles range from 105.2(2) to 111.7(3)°. The terminal V–O^{Me} bonds are significantly longer than the V– μO^{Ni} bonds (average V–O^{Me} = 1.621(5) Å vs average V– μO^{Ni} 1.791(7) Å).

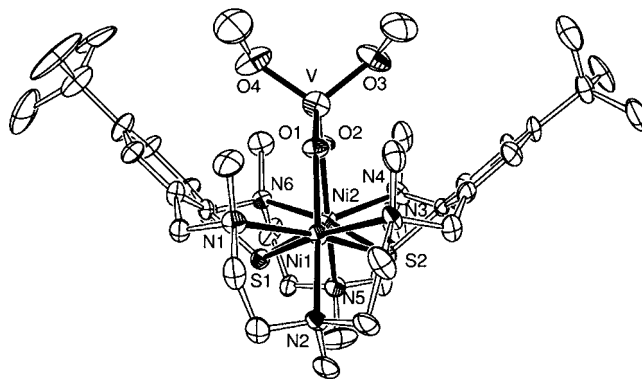


Figure 4. Structure of the $[\text{Ni}_2\text{L}(\mu\text{-O}_2\text{V}(\text{OMe})_2)]^+$ cation in crystals of **3BPh₄·xMeCN**.³¹ Thermal ellipsoids are drawn at the 30% probability level. Hydrogen atoms are omitted for reasons of clarity.

Table 4. Selected Bond Lengths [Å] in Complexes 3–7

| L' | 3 | 4 | 5 | 6 | 7 |
|-------------------|--|--|---|---|---|
| | $[\text{O}_2\text{V}(\text{OMe})_2]^-$ | $[\text{O}_2\text{V}(\text{OEt})_2]^-$ | $[\text{O}_2\text{V}(\text{OH})(\text{O}(\text{CH}_2)_2\text{OH})]^-$ | $[\text{O}_2\text{V}((\text{OCH}_2)_2\text{CH}_2)]^-$ | $[\text{O}_2\text{V}((\text{OCH}_2\text{CH}_2)_2\text{O})]^-$ |
| V–O1 | 1.627(5) | 1.566(3) | 1.586(5) | 1.622(2) | 1.579(5) |
| V–O2 | 1.615(5) | 1.601(3) | 1.572(5) | 1.615(2) | 1.541(5) |
| V–O3 | 1.757(6) | 1.686(7) | 1.721(10) | 1.776(3) | 1.866(12) |
| V–O4 | 1.825(7) | 1.806(6) | 1.780(11) | 1.775(3) | 1.868(11) |
| O1–V–O2 | 105.2(2) | 104.88(17) | 104.8(3) | 108.50(13) | 102.0(3) |
| O1–V–O3 | 113.6(3) | 111.2(2) | 111.5(4) | 114.59(17) | 109.0(5) |
| O1–V–O4 | 111.7(3) | 110.3(2) | 114.2(5) | 112.11(15) | 103.6(5) |
| O2–V–O3 | 108.2(3) | 111.1(2) | 114.2(4) | 110.71(15) | 112.0(4) |
| O2–V–O4 | 111.4(3) | 115.0(3) | 111.0(4) | 111.01(15) | 115.0(5) |
| O3–V–O4 | 106.8(3) | 104.6(3) | 101.3(6) | 99.76(19) | 113.9(5) |
| Ni1–O1 | 2.034(5) | 2.036(3) | 2.012(5) | 2.045(2) | 2.003(5) |
| Ni1–N1 | 2.276(6) | 2.264(4) | 2.225(6) | 2.209(3) | 2.233(6) |
| Ni1–N2 | 2.142(6) | 2.154(4) | 2.149(6) | 2.150(3) | 2.151(7) |
| Ni1–N3 | 2.279(6) | 2.271(4) | 2.263(6) | 2.257(3) | 2.270(6) |
| Ni1–S1 | 2.477(2) | 2.436(1) | 2.449(2) | 2.4556(12) | 2.446(2) |
| Ni1–S2 | 2.431(2) | 2.475(1) | 2.486(2) | 2.4844(11) | 2.480(2) |
| Ni2–O2 | 2.024(5) | 2.024(3) | 2.010(5) | 2.016(3) | 2.021(5) |
| Ni2–N4 | 2.216(7) | 2.264(4) | 2.274(6) | 2.255(3) | 2.281(7) |
| Ni2–N5 | 2.150(6) | 2.148(3) | 2.146(7) | 2.129(3) | 2.154(6) |
| Ni2–N6 | 2.276(6) | 2.240(4) | 2.255(6) | 2.260(3) | 2.258(6) |
| Ni2–S1 | 2.466(2) | 2.465(1) | 2.428(2) | 2.4312(12) | 2.425(2) |
| Ni2–S2 | 2.466(2) | 2.476(1) | 2.475(2) | 2.4883(11) | 2.472(2) |
| Ni–N ^a | 2.230(6) | 2.224(4) | 2.219(6) | 2.210(3) | 2.224(7) |
| Ni–O ^a | 2.029(5) | 2.030(3) | 2.011(5) | 2.033(2) | 2.012(6) |
| Ni–S ^a | 2.460(2) | 2.463(1) | 2.456(2) | 2.4649(12) | 2.456(2) |
| Ni1...Ni2 | 3.585(1) | 3.578(1) | 3.563(1) | 3.604(1) | 3.528(1) |
| Ni1...V | 3.443(1) | 3.408(1) | 3.418(1) | 3.443(1) | 3.421(1) |
| Ni2...V | 3.458(1) | 3.444(1) | 3.393(1) | 3.412(1) | 3.396(1) |

^aAverage values.

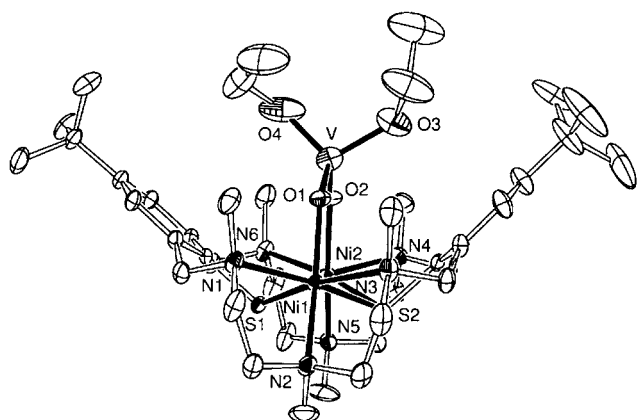


Figure 5. Structure of the $[\text{Ni}_2\text{L}(\mu\text{-VO}_2(\text{OEt})_2)]^+$ cation in crystals of $4\text{BPh}_4 \cdot x\text{MeCN}$. Thermal ellipsoids are drawn at the 30% probability level. Hydrogen atoms are omitted for reasons of clarity.

This situation is normal for low-coordinate oxovanadium(V) alkoxides. In dimeric $\{[\text{VO}(\text{OC}_5\text{H}_9)_3]_2\}$,³⁸ for example, with a $(\text{RO})_2(\text{O})\text{V}(\mu\text{OR})_2\text{V}(\text{O})(\text{OR})_2$ unit, the V–O bonds are 1.595(3) Å (V=O), 1.835(4) Å (V– μOR), 1.762(3) Å, 1.763(6) Å (V–OR), and 2.296 Å (V– μOR).

There are no unusual features as far as bond lengths and angles in the $[\text{Ni}_2\text{L}]^{2+}$ fragments are concerned. The average Ni– μ -S (2.460(2) Å), Ni–N (2.230(6) Å), and Ni– μ -O (2.029(5) Å) bond lengths are similar to other biocatahedral $[\text{Ni}_2\text{L}(\text{L}')^+]^+$ complexes.^{72,28} The M···M distances are 3.585(1) Å (Ni1···Ni2), 3.443(1) Å (Ni1···V), and 3.458(1) Å (Ni2···V).

To our knowledge there exist only few examples of structurally characterized tetrahedral oxo-alkoxo vanadates. Kitagawa has described a mixed-valence tetranuclear vanadium(IV,V) complex, $[\text{V}_4\text{O}_4(\mu\text{-OEt})_2(\mu\text{-O})_2(\text{OEt})_4(\text{phen})_2]$, in which two four-coordinate $[\text{VO}_2(\text{OEt})_2]^-$ moieties are μ -oxo-bridged to a dinuclear $[\text{V}_2\text{O}_2(\mu\text{-OEt})_2]^{2+}$ unit.³⁷ The V=O, V–OEt, and V– μ O bond lengths of this unit are at 1.601(3) Å, 1.771(4) Å, and 1.670(3) Å, respectively, similar to the respective bond lengths in **4**. Neutral $\text{VO}(\text{OR})_3$ alkyl esters tend to oligomerize in the solution as well as in the solid state forming five- or hexa-coordinate V^{V} compounds. The stabilization of the $\text{VO}_2(\text{OMe})_2^-$ and $\text{VO}_2(\text{OEt})_2^-$ units can be attributed to the steric protection offered by the bowl-shaped conformation of the supporting ligand of the $[\text{Ni}_2\text{L}]^{2+}$ complex.

$[\text{Ni}_2\text{L}(\mu\text{-O}_2\text{V}(\text{OH})(\text{OCH}_2\text{CH}_2\text{OH}))]\text{BPh}_4 \cdot x\text{MeCN}$ (**5BPh₄·xMeCN**).⁸¹ Crystals of **5BPh₄·xMeCN** suitable for X-ray crystallography were grown by recrystallization from MeCN. Compound **5BPh₄·xMeCN** crystallizes in the triclinic space group $P\bar{1}$. The crystal structure of **5BPh₄·xMeCN** is composed of $[\text{Ni}_2\text{L}(\mu\text{-O}_2\text{V}(\text{OH})(\text{OCH}_2\text{CH}_2\text{OH}))]^+$ cations, tetraphenylborate anions, and disordered acetonitrile solvate molecules. Figure 6 shows a perspective view of the structure of the $[\text{Ni}_2\text{L}(\mu\text{-O}_2\text{V}(\text{OH})(\text{OCH}_2\text{CH}_2\text{OH}))]^+$ cation. Selected bond lengths and angles are given in Table 4.

The crystal structure confirms the presence of an acyclic monoester. The 2-hydroxyethyl vanadate has an intramolecular hydrogen bond with the terminal V–OH unit, as suggested by the O4···O5 distance of 2.797 Å. The $[\text{O}_2\text{V}(\text{OH})(\text{OCH}_2\text{CH}_2\text{OH})]^-$ group is distorted from an ideal tetrahedral geometry. The V–O^{alkyl} (1.72(1) Å) and the V–OH (1.78(1) Å) bonds are longer than the V– μO^{Ni} (mean 1.579(5) Å) bonds. The O–V–O bond angles deviate by as much as 8° from their

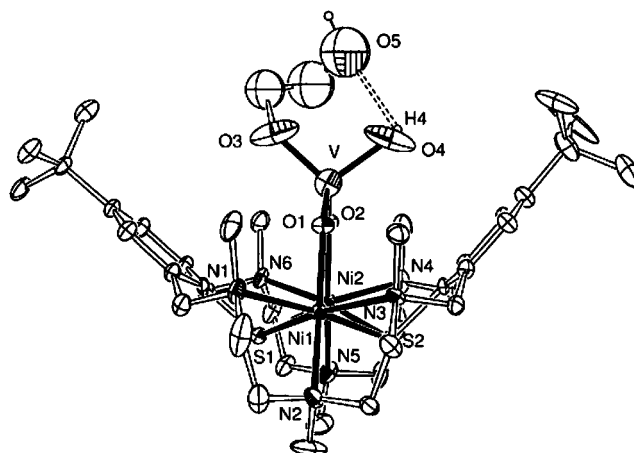


Figure 6. Structure of the $[\text{Ni}_2\text{L}(\mu\text{-VO}_2(\text{OH})(\text{OCH}_2\text{CH}_2\text{OH}))]^+$ cation in crystals of $5\text{BPh}_4 \cdot x\text{MeCN}$. Thermal ellipsoids are drawn at the 30% probability level. Hydrogen atoms, except H4 and H5a, are omitted for reasons of clarity. The dashed bond indicates a hydrogen bonding interaction, O4···O5 2.797 Å.

ideal values. It should be noted that the free $[\text{O}_2\text{V}(\text{OH})(\text{OCH}_2\text{CH}_2\text{OH})]^-$ ion has been detected by ⁵¹V NMR spectroscopy,⁷⁰ but has never been isolated in its free form.

$[\text{Ni}_2\text{L}(\mu\text{-O}_2\text{V}(\text{OCH}_2)_2\text{CH}_2)]\text{BPh}_4 \cdot x\text{MeCN}$ (**6BPh₄·xMeCN**).⁸¹ The macrocycle adopts a bowl-shaped conformation, as observed in complexes **3–5**. Each nickel atom is coordinated by two S and three N atoms from the supporting ligand and an O atom of a $\mu_{1,3}$ -bridging $[\text{O}_2\text{V}(\text{OCH}_2)_2\text{CH}_2]^-$ ion in a severely distorted octahedral fashion (Figure 7). The

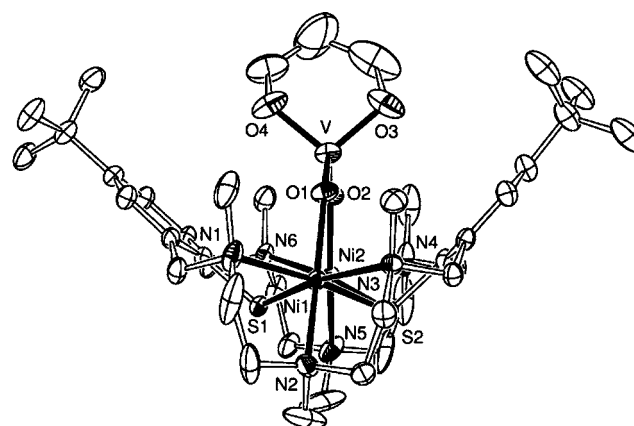


Figure 7. Structure of the $[\text{Ni}_2\text{L}(\mu\text{-O}_2\text{V}(\text{OCH}_2)_2\text{CH}_2)]^+$ cation in crystals of $6\text{BPh}_4 \cdot n\text{MeCN}$. Thermal ellipsoids are drawn at the 30% probability level. Hydrogen atoms are omitted for reasons of clarity.

1,3-propane diolate chelates the pseudo tetrahedral vanadium atom forming a six-membered ring. The mean V– μONi (1.619(2) Å) and V–O^{alkyl} (1.776(3) Å) bond lengths differ by about 0.16 Å and the O–V–O bond angles range from 99.8(1)° to 114.6(2)°. The O3–V–O4 angle in **6** at 99.8(1)° is significantly smaller than in **3–5**. This bond angle contraction can be attributed to the bonding constraints of the 1,3-propane diolate ligand. The Ni–ligand bond lengths in **6** are very similar to those in **3–5**.

$[\text{Ni}_2\text{L}(\mu\text{-O}_2\text{V}(\text{OCH}_2\text{CH}_2)_2\text{O})]\text{BPh}_4 \cdot x\text{MeCN}$ ($7\text{BPh}_4 \cdot x\text{MeCN}$).⁸¹ Crystals of $7\text{BPh}_4 \cdot x\text{MeCN}$ suitable for X-ray crystallography were grown by recrystallization from MeCN. Figure 8 displays

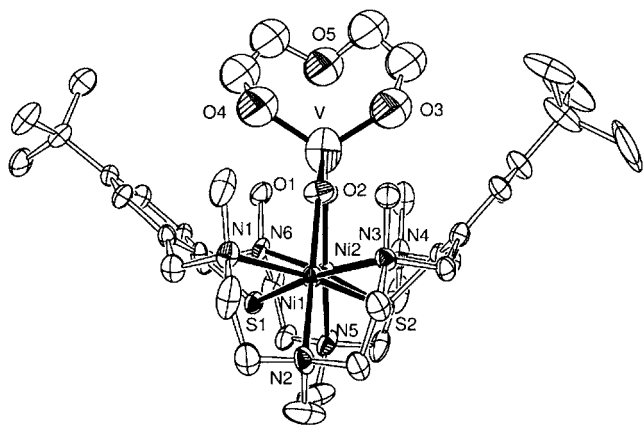


Figure 8. Structure of the $[\text{Ni}_2\text{L}(\mu\text{-O}_2\text{V}(\text{OCH}_2\text{CH}_2)_2\text{O})]^+$ cation in crystals of $7\text{BPh}_4 \cdot x\text{MeCN}$. Thermal ellipsoids are drawn at the 30% probability level. Hydrogen atoms are omitted for reasons of clarity.

an ORTEP representation of the $[\text{Ni}_2\text{L}(\mu\text{-O}_2\text{V}(\text{OCH}_2\text{CH}_2)_2\text{O})]^+$ cation. The vanadium is chelated by the diethylene glycol unit, but the ether oxygen remains uncoordinated ($\text{V}\cdots\text{O}(5)$ 2.925(3) Å), providing support that a five-coordinate vanadate complex cannot be accommodated within the binding pocket of $[\text{Ni}_2\text{L}]^{2+}$. The $[\text{O}_2\text{V}(\text{OCH}_2\text{CH}_2)_2\text{O}]^-$ unit in **7** is less distorted from tetrahedral symmetry than **6**. The $[\text{Ni}_2\text{L}]^{2+}$ subunit in **7** and **3–6** are structurally very similar, and the Ni–N and Ni–S distances lie within very narrow ranges.

CONCLUDING REMARKS

The main findings of the present work can be summarized as follows: (i) A series of isostructural $[\text{Ni}^{\text{II}}\text{L}(\mu\text{-O}_2\text{V}(\text{OR})_2)]^+$ complexes bearing vanadate ($\text{R} = \text{H}$) and vanadate esters as coligands have been prepared. (ii) The vanadate complex $[\text{Ni}_2\text{L}(\mu\text{-O}_2\text{V}(\text{OH})_2)]^+$ **2** is only accessible in aprotic solvents. In alcohols, **2** is readily esterified to generate $[\text{Ni}_2(\mu\text{-O}_2\text{V}(\text{OR})_2)]^+$ complexes bearing acyclic ($\text{R} = \text{Me}$ (**3**), Et (**4**)) or cyclic vanadate diesters ($\text{R} = 1,3\text{-CH}_2\text{CH}_2\text{CH}_2$ (**6**), $\text{CH}_2\text{CH}_2\text{-O-CH}_2\text{CH}_2$ (**7**)) or monoesters ($\text{R} = \text{-CH}_2\text{CH}_2\text{OH}$ (**5**)). (iii) The vanadate diesters can be prepared by several methods, of which esterification of **2** or transesterification of **3** represent the methods of choice. (iv) The esterification reactions are believed to proceed outside the binding pocket of the complexes, given that there is not enough room to accommodate a five-coordinate intermediate (according to CPK models and the fact that the ether oxygen donor of the diethylene glycol unit in **7** remains uncoordinated). (v) The present esterification and transesterification reactions are less complex than the unconstrained reactions between alcohols and vanadates, and are selective for the four-coordinate vanadate diesters. This is attributable to a thermodynamic template effect played by the $[\text{Ni}_2\text{L}]^{2+}$ fragment, which can only accommodate the four-coordinate $[\text{O}_2\text{V}(\text{OR})_2]^-$ esters in its binding pocket. (vi) The $\text{O}_2\text{V}(\text{OMe})_2^-$ unit in **3** is redox inactive in a potential window from -2.0 to $+2.5$ V vs SCE. (vii) Finally, the spins of the nickel(II) ($S_i = 1$ ions) in **3** are

weakly ferromagnetically coupled ($J = +23 \text{ cm}^{-1}$, ($\text{H} = -2J\text{S}_1\text{S}_2$)) to produce an $S = 2$ ground state.

Current studies in this laboratory focus on transesterification reactions of **2** with other alcohols such as triols and carbohydrates. We also plan studies with the diamagnetic $[\text{Zn}_2\text{L}]^{2+}$ fragment to investigate these reactions in solution by NMR spectroscopy.

ASSOCIATED CONTENT

Supporting Information

X-ray crystallographic data in CIF format. Experimental and calculated susceptibility data for 3BPh_4 . This material is available free of charge via the Internet at <http://pubs.acs.org>.

AUTHOR INFORMATION

Corresponding Author

*E-mail: b.kersting@uni-leipzig.de. Fax: +49/(0)341-97-36199.

Present Address

[†]Laboratory of Coordination Chemistry, Institute of Chemistry, Academy of Sciences of Moldova, Academiei str. 3, MD-2028 Chisinau, Republic Moldova.

Notes

The authors declare no competing financial interest.

ACKNOWLEDGMENTS

This work was supported by the Deutsche Forschungsgemeinschaft (Graduate school Building with Molecules and Nano-objects, “BuildMona”; DFG-FOR 1154 “Towards molecular spintronics”) and the University of Leipzig. J.L. thanks the SAB for an ESF grant.

REFERENCES

- (1) Kersting, B.; Lehmann, U. In *Advances in Inorganic Chemistry*; van Eldik, R., Hubbard, C. D., Eds.; Academic Press: New York, 2009; Vol. 61, pp 407–470.
- (2) Kersting, B. In *Activating Unreactive Molecules - The Role of secondary Interactions*; Bolm, C., Hahn, F. E., Eds.; Wiley-VCH: Weinheim, Germany, 2009; Chapter 1, pp 1–17.
- (3) Gibb, C. L. D.; Gibb, B. C. *J. Am. Chem. Soc.* **2004**, *126*, 11408–11409.
- (4) Breslow, R. *Acc. Chem. Res.* **1995**, *28*, 146–153.
- (5) Canary, J. W.; Gibb, B. C. *Prog. Inorg. Chem.* **1997**, *45*, 1–81.
- (6) Armspach, D.; Matt, D. *Chem. Commun.* **1999**, 1073–1074.
- (7) Cameron, B. R.; Loeb, S. J.; Yap, G. P. *Inorg. Chem.* **1997**, *36*, 5498–5504.
- (8) Reetz, M. T.; Waldvogel, S. R. *Angew. Chem.* **1997**, *109*, 870–873; *Angew. Chem., Int. Ed. Engl.* **1997**, *36*, 865–867.
- (9) Molenveld, P.; Engbersen, J. F. J.; Reinhoudt, D. N. *Chem. Soc. Rev.* **2000**, *29*, 75–86.
- (10) S n que, O.; Campion, M.; Giorgi, M.; Le Mest, Y.; Reinaud, O. *Eur. J. Inorg. Chem.* **2004**, 1817–1826.
- (11) Breslow, R., Ed.; *Artificial Enzyme*; Wiley-VCH: Weinheim, Germany, 2005.
- (12) Merlau, M. L.; Del Pilar Mejia, M.; Nguyen, S. T.; Hupp, J. T. *Angew. Chem.* **2001**, *113*, 4369–4372; *Angew. Chem., Int. Ed.* **2001**, *40*, 4239–4242.
- (13) Hammes, B. S.; Ramos-Maldonado, D.; Yap, G. P. A.; Liable-Sands, L.; Rheingold, A. L.; Young, V. G., Jr.; Borovik, A. S. *Inorg. Chem.* **1997**, *36*, 3210–3211.
- (14) Pilkington, N. H.; Robson, R. *Aust. J. Chem.* **1970**, *23*, 2225–2236.
- (15) (a) Vigato, P. A.; Tamburini, S.; Fenton, D. *Coord. Chem. Rev.* **1990**, *106*, 25–170. (b) Fenton, D. *Chem. Soc. Rev.* **1999**, *28*,

- 159–168. (c) Yamami, M.; Furutachi, H.; Yokoyama, T.; Okawa, H. *Inorg. Chem.* **1998**, *37*, 6832–6838. (d) Okawa, H.; Furutachi, H.; Fenton, D. E. *Coord. Chem. Rev.* **1998**, *174*, 51–75. (e) Shinoura, M.; Kita, S.; Ohba, M.; Okawa, H.; Furutachi, H.; Suzuki, M. *Inorg. Chem.* **2000**, *39*, 4520–4526.
- (16) (a) Atkins, A. J.; Blake, A. J.; Schröder, M. *J. Chem. Soc., Chem. Commun.* **1993**, 1662–1665. (b) Branscombe, N. D. J.; Blake, A. J.; Marin-Becerra, A.; Li, W.-S.; Parsons, S.; Ruiz-Ramirez, L.; Schröder, M. *J. Chem. Soc., Chem. Commun.* **1996**, 2573–2574.
- (17) (a) Brooker, S.; Croucher, P. D. *J. Chem. Soc., Chem. Commun.* **1995**, 1493–1494. (b) Brooker, S.; Croucher, P. D. *J. Chem. Soc., Chem. Commun.* **1995**, 2075–2076. (c) Brooker, S.; Croucher, P. D.; Roxburgh, F. M. *J. Chem. Soc., Dalton Trans.* **1996**, 3031–3037. (d) Brooker, S.; Croucher, P. D. *J. Chem. Soc., Chem. Commun.* **1997**, 459–460.
- (18) (a) Kersting, B.; Steinfeld, G. *Chem. Commun.* **2001**, 1376–1377. (b) Klingele, M. H.; Steinfeld, G.; Kersting, B. *Z. Naturforsch.* **2001**, *56b*, 901–907.
- (19) Kersting, B. *Z. Anorg. Allg. Chem.* **2004**, *630*, 765–780.
- (20) Lozan, V.; Loose, C.; Kortus, J.; Kersting, B. *Coord. Chem. Rev.* **2009**, *253*, 2244–2260.
- (21) Kersting, B. *Angew. Chem.* **2001**, *113*, 4109–4112; *Angew. Chem., Int. Ed.* **2001**, *40*, 3987–3990.
- (22) Steinfeld, G.; Lozan, V.; Kersting, B. *Angew. Chem.* **2003**, *115*, 2363–2365; *Angew. Chem., Int. Ed.* **2003**, *42*, 2261–2263.
- (23) Käss, S.; Gregor, T.; Kersting, B. *Angew. Chem.* **2006**, *118*, 107–110; *Angew. Chem., Int. Ed.* **2006**, *45*, 101–104.
- (24) Lozan, V.; Kersting, B. *Inorg. Chem.* **2008**, *47*, 5386–5393.
- (25) Journaux, Y.; Lozan, V.; Hausmann, J.; Kersting, B. *Chem. Commun.* **2006**, 83–84.
- (26) Lozan, V.; Kersting, B. *Eur. J. Inorg. Chem.* **2007**, 1436–1443.
- (27) Lozan, V.; Kersting, B. *Inorg. Chem.* **2006**, *45*, 5630–5634.
- (28) Steinfeld, G.; Kersting, B. *Z. Anorg. Allg. Chem.* **2009**, *635*, 260–264.
- (29) Crans, D. C. *Pure Appl. Chem.* **2005**, *77*, 1497–1527.
- (30) Zubieta, J.; Chen, Q. *Coord. Chem. Rev.* **1992**, *114*, 107–167.
- (31) Gibson, V. C.; Redshaw, C.; Elsegood, M. R. J. *J. Chem. Soc., Dalton Trans.* **2001**, 767–769.
- (32) Hou, D.; Hagen, K. S.; Hill, C. L. *J. Am. Chem. Soc.* **1992**, *114*, 5864–5866.
- (33) Rehder, D. *Angew. Chem.* **1991**, *103*, 152–172; *Angew. Chem., Int. Ed. Engl.* **1991**, *30*, 148–167.
- (34) Priesch, W.; Rehder, D. *Inorg. Chem.* **1990**, *29*, 3013–3019.
- (35) Spandl, J.; Brüdgam, I.; Hartl, H. *Z. Anorg. Allg. Chem.* **2000**, *626*, 2125–2132.
- (36) Henderson, R. A.; Hughes, D. L.; Janas, Z.; Richards, R. L.; Sobota, P.; Szafert, S. *J. Organomet. Chem.* **1998**, *554*, 195–201.
- (37) Kumagai, H.; Endo, M.; Kawata, S.; Kitagawa, S. *Acta Crystallogr.* **1996**, *C52*, 1943–1945.
- (38) Hillerns, F.; Olbrich, F.; Behrens, U.; Rehder, D. *Angew. Chem.* **1992**, *104*, 479–480; *Angew. Chem., Int. Ed. Engl.* **1992**, *31*, 447–448.
- (39) Crans, D. C. In *Metal Ions in Biological Systems*; Sigel, H., Sigel, A., Eds.; Marcel Dekker: New York, 1995; Vol. 31, pp 147–209.
- (40) Crans, D. C.; Trujillo, A. M.; Pharażyna, P. S.; Cohen, M. D. *Coord. Chem. Rev.* **2011**, *255*, 2178–2192.
- (41) Cormman, C. R.; Kampf, J.; Lah, M. S.; Pecoraro, V. L. *Inorg. Chem.* **1992**, *31*, 2035–2043.
- (42) Rehder, D. *Bioinorganic Vanadium Chemistry*; John Wiley & Sons: New-York, 2008.
- (43) Waters, T.; Khairallah, G. N.; Wimala, S. A. S. Y.; Ang, Y. C.; O'Hair, R. A. J.; Wedd, A. G. *Chem. Commun.* **2006**, 4503–4505.
- (44) Borah, B.; Chen, C. W.; Egan, W.; Miller, M.; Wlodawer, A.; Cohen, J. S. *Biochemistry* **1985**, *24*, 2058–2067.
- (45) Rehder, D.; Holst, H.; Quaas, R.; Hinrichs, W.; Hahn, U.; Saenger, W. *J. Inorg. Biochem.* **1989**, *37*, 141–150.
- (46) Kozlov, Y. N.; Romakh, V. B.; Kitaygorodskiy, A.; Buglyo, P.; Süss-Fink, G.; Shul'pin, G. B. *J. Phys. Chem. A* **2007**, *111*, 7736–7752.
- (47) SADABS, an empirical absorption correction program, part of the SAINTPlus NT version 5.10 package; Bruker AXS: Madison, WI, 1998.
- (48) Sheldrick, G. M. *Acta Crystallogr.* **1990**, *A46*, 467–473.
- (49) Sheldrick, G. M. *SHELXL-97*, Computer program for crystal structure refinement; University of Göttingen: Göttingen, Germany, 1997.
- (50) *ShelXTL*, version 5.10; Bruker AXS: Madison, WI, 1998.
- (51) Spek, A. L. *PLATON - A Multipurpose Crystallographic Tool*; Utrecht University: Utrecht, The Netherlands, 2000.
- (52) Farrugia, L. J. *J. Appl. Crystallogr.* **1997**, *30*, 565.
- (53) Sluis, P.; v.d.; Spek, A. L. *Acta Crystallogr.* **1990**, *A46*, 194.
- (54) Under our experimental conditions $E(\text{Cp}_2\text{Co}^+/\text{Cp}_2\text{Co}) = -1.345 \text{ V vs } E(\text{Cp}_2\text{Fe}^+/\text{Cp}_2\text{Fe})$; $E(\text{Cp}_2\text{Co}^+/\text{Cp}_2\text{Co}) = -0.937 \text{ V vs SCE}$. Connelly, N. G.; Geiger, W. E. *Chem. Rev.* **1996**, *96*, 877–910.
- (55) Funk, H.; Weiss, W.; Zeising, M. *Z. Anorg. Allg. Chem.* **1958**, *296*, 36–45.
- (56) Mittal, R. K.; Mehrotra, R. C. *Z. Anorg. Allg. Chem.* **1964**, *327*, 311–314.
- (57) Sekiguchi, S.; Kurihara, A. *Bull. Chem. Soc. Jpn.* **1969**, *42*, 1453–1454.
- (58) Crans, D. C.; Schelble, S. M.; Theisen, L. A. *J. Org. Chem.* **1991**, *56*, 1266–1274.
- (59) Tracey, A. S.; Leon-Lai, C. H. *Inorg. Chem.* **1991**, *30*, 3200–3204.
- (60) Tracey, A. S.; Gresser, M. J. *Can. J. Chem.* **1988**, *66*, 2570–2574.
- (61) Gresser, M. J.; Tracey, A. S. *J. Am. Chem. Soc.* **1985**, *107*, 4215–4220.
- (62) Jiang, F.; Anderson, O. P.; Miller, S. M.; Chen, J.; Mahroof-Tahir, M.; Crans, D. C. *Inorg. Chem.* **1998**, *37*, 5439–5451.
- (63) Crans, D. C.; Jiang, F.; Chen, J.; Andersen, O. P.; Miller, M. M. *Inorg. Chem.* **1997**, *36*, 1038–1047.
- (64) Yoshizawa, M.; Kusakawa, T.; Fujita, M.; Yamaguchi, K. *J. Am. Chem. Soc.* **2000**, *122*, 6311–6312.
- (65) Bertini, I.; Luchinat, C.; Parigi, G. Solution NMR of Paramagnetic Molecules, Applications to Metallobiomolecules and Model. In *Current Methods in Inorganic Chemistry*; Elsevier: Amsterdam, The Netherlands, 2001; Vol. 2, Chapter 6.
- (66) Crans, D. C.; Chen, H. J.; Felty, R. A. *J. Am. Chem. Soc.* **1992**, *114*, 4543–4550.
- (67) Crans, D. C.; Felty, R. A.; Miller, M. M. *J. Am. Chem. Soc.* **1991**, *113*, 265–269.
- (68) Crans, D. C.; Felty, R. A.; Anderson, O. P.; Miller, M. M. *Inorg. Chem.* **1993**, *32*, 247–248.
- (69) Crans, D. C.; Felty, R. A.; Chen, H.; Eckert, H.; Das, N. *Inorg. Chem.* **1994**, *33*, 2427–2438.
- (70) Gresser, M. J.; Tracey, A. S. *J. Am. Chem. Soc.* **1986**, *108*, 1935–1939.
- (71) Hambley, T. W.; Judd, R. J.; Lay, P. A. *Inorg. Chem.* **1992**, *31*, 343–345.
- (72) Lee, K.; Lozan, V.; Langford, S.; Kersting, B. *Dalton Trans.* **2009**, 7481–7485.
- (73) Journaux, Y.; Glaser, T.; Steinfeld, G.; Lozan, V.; Kersting, B. *Dalton Trans.* **2006**, 1738–1748.
- (74) Kahn, O. *Molecular Magnetism*; VCH-Wiley: New York, 1993.
- (75) Azuah, R. T.; Kneller, L. R.; Qiu, Y.; Tregenna-Piggott, P. L. W.; Brown, C. M.; Copley, J. R. D.; Dimeo, R. M. *J. Res. Natl. Inst. Stand. Technol.* **2009**, *114*, 341–358.
- (76) Boča, R.; Dlháň, L.; Haase, W.; Herchel, R.; Mašlejová, A.; Papánková, B. *Chem. Phys. Lett.* **2003**, *373*, 402–410.
- (77) Mukherjee, P.; Drew, M. G.; Tangoulis, V.; Estrader, M.; Diaz, C.; Ghosh, A. *Polyhedron* **2009**, *28*, 2989–2996.
- (78) Carlin, R. L. *Magnetochemistry*; Springer: Berlin, Germany, 1986; pp 12–13.
- (79) Nanda, K. K.; Addison, A. W.; Paterson, N.; Sinn, E.; Thompson, L. K.; Sakaguchi, U. *Inorg. Chem.* **1998**, *37*, 1028–1036.
- (80) Lach, J.; Hahn, T.; Kersting, B.; Kortus, J. *Eur. J. Inorg. Chem.* **2012**, *14*, 2381–2388.

(81) The acetonitrile solvate molecules in all complexes are heavily disordered, and the exact number of the solvate molecules could not be determined. Electron density attributed to the disordered acetonitrile molecules was removed from the structures, see Experimental Section.